Supplemental Information

Transcriptional changes during naturally-acquired Zika Virus infection render dendritic cells highly conducive to viral replication

Xiaoming Sun[1,4], Stephane Hua[1,4], Hsiao-Rong Chen[1], Zhengyu Ouyang[1], Kevin Einkauf[1], Samantha Tse[1], Kevin Ard[3], Andrea Ciaranello[3], Sigal Yawetz[2], Paul Sax[2], Eric S. Rosenberg[3], Mathias Lichterfeld[1,2], Xu G. Yu[1,2,*]

Figure S1

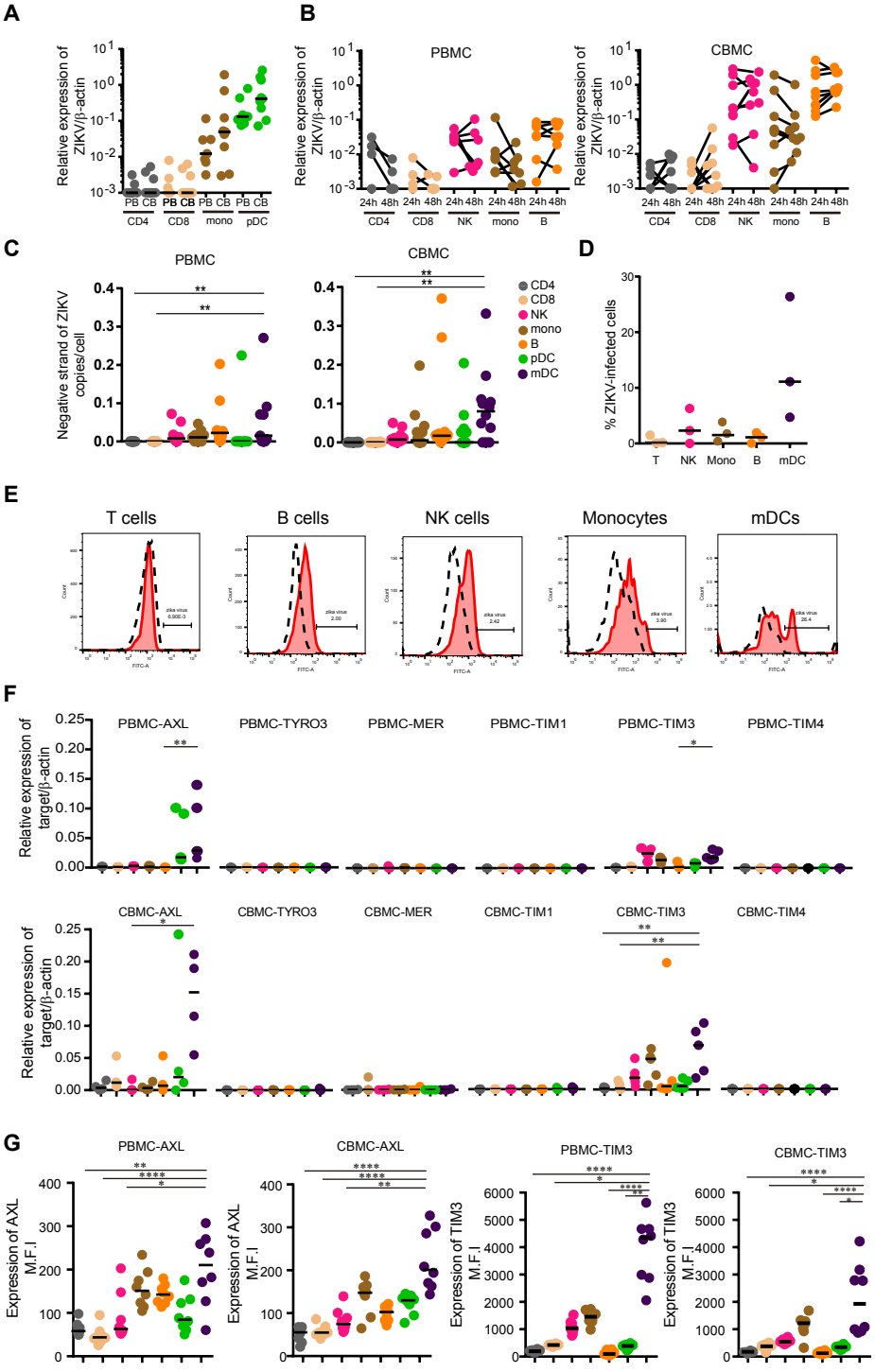
A
B
C
D
E
F
G
Relative expression of ZIKV/β-actin
PB CB PB CB PB CB PB CB
CD4 CD8 mono pDC
PBMC
CBMC
24h 48h
CD4 CD8 NK mono B
Negative strand of ZIKV copies/cell
CD4
CD8
NK
mono
B
pDC
mDC
% ZIKV-infected cells
T NK Mono B mDC
T cells
B cells
NK cells
Monocytes
mDCs
Relative expression of target/β-actin
PBMC-AXL
PBMC-TYRO3
PBMC-MER
PBMC-TIM1
PBMC-TIM3
PBMC-TIM4
CBMC-AXL
CBMC-TYRO3
CBMC-MER
CBMC-TIM1
CBMC-TIM3
CBMC-TIM4
Expression of AXL M.F.I
Expression of TIM3 M.F.I

Figure S1, related to Figure 1. ZIKV infect PBMCs and CBMCs and its potential entry receptors.

(A) PBMCs and CBMCs were infected for 24hours with ZIKV at MOI of 1 followed by sorting of CD4 T cells, CD8 T cells, NK, Monocytes, B cells, pDCs, and mDCs. Viral replication was measured by qRT-PCR. The levels of viral replication in CD4 cells, CD8 T cells, monocytes and pDCs from PBMCs and CBMCs were compared.

(B) PBMCs and CBMCs were infected with ZIKV at MOI of 1, followed by sorting of CD4 T cells, CD8 T cells, NK, Monocytes, B cells, pDCs, and mDCs at 24 and 48hours post-infection. Viral replication was measured by qRT-PCR.

(C) PBMCs and CBMCs were infected with ZIKV at MOI of 1, followed by sorting of CD4 T cells, CD8 T cells, NK, Monocytes, B cells, pDCs, and mDCs at 24 post-infection. Negative-stranded Zika RNA was determined by qPCR and compared in subsets from PBMCs (left) and CBMCs (right).

(**D**) Proportion of indicated cells expressing ZIKV E protein after *in vitro* infection. Data from 3 experiments are shown.

(**E**) Representative histograms reflecting expression of the ZIKV E protein following infection of sorted cells with ZIKV (MOI = 1) for 48h or 72h. Results from mock-infected cells (dashed lines) are shown for comparison.

(F) Analysis of host RNA encoding for potential entry receptors for Zika virus during *in vitro* ZIKV infection. mRNA expression levels of AXL, TYRO3, MER, TIM1, TIM3, and TIM4 were measured by qPCR in both PBMCs (upper panel) and CBMCs (lower panel).

(G) Protein expression level of AXL (left panel) and TIM3 (right panel) were measured by flow cytometry in indicated cell subsets from both PBMCs and CBMCs.

Horizontal lines reflect the median. Intra-individual differences were tested for statistical significance using Friedman test with post-hoc Dunn's test; * $p<0.05$; ** $p<0.01$; *** $p < 0.001$; **** $p< 0.0001$.

Figure S2

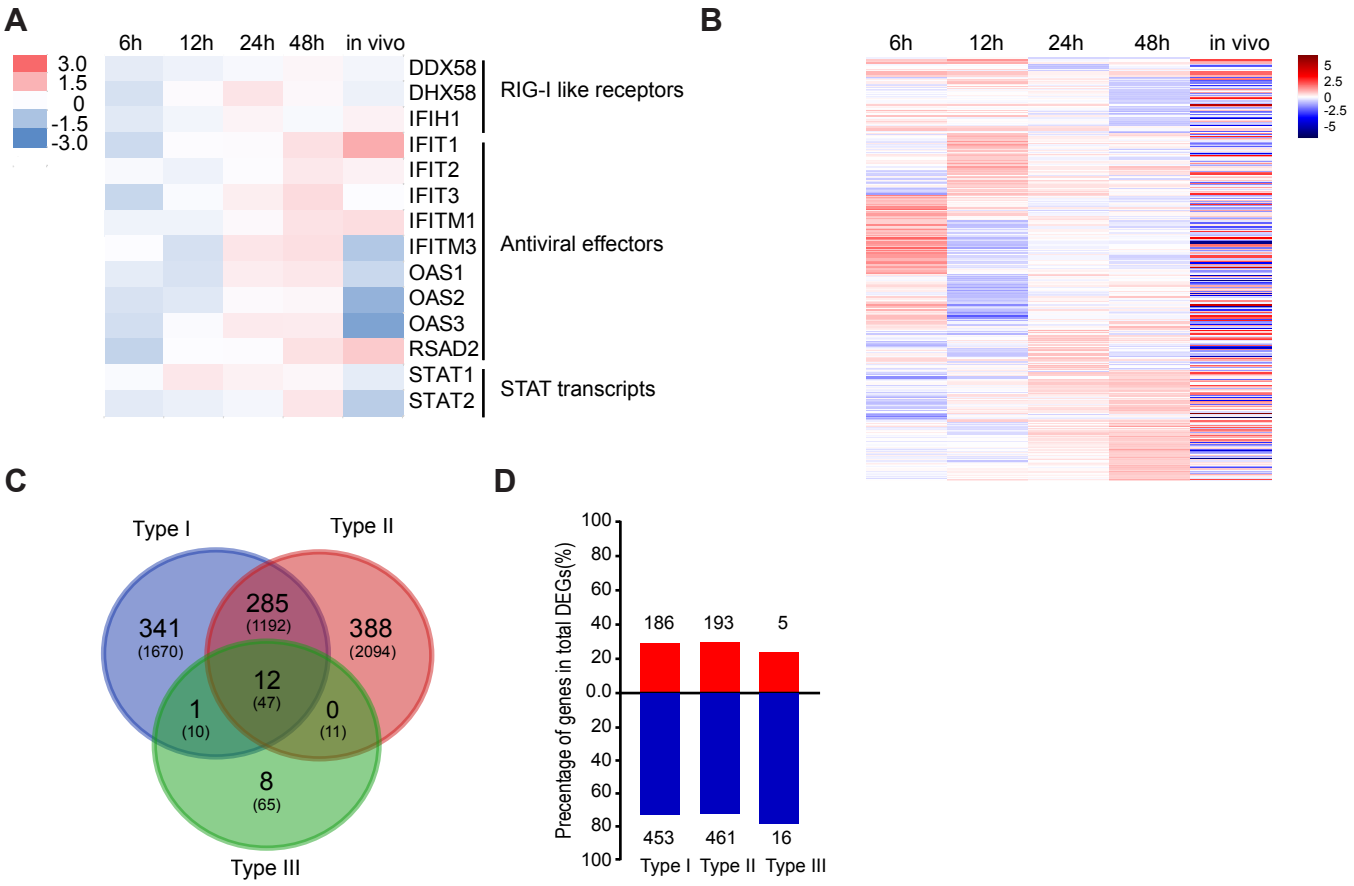
A
6h
12h
24h
48h
in vivo
3.0
1.5
0
-1.5
-3.0
DDX58
DHX58
IFIH1
IFIT1
IFIT2
IFIT3
IFITM1
IFITM3
OAS1
OAS2
OAS3
RSAD2
STAT1
STAT2
RIG-I like receptors
Antiviral effectors
STAT transcripts
B
6h
12h
24h
48h
in vivo
5
2.5
0
-2.5
-5
C
Type I
Type II
Type III
341
(1670)
285
(1192)
388
(2094)
12
(47)
1
(10)
0
(11)
8
(65)
D
Precentage of genes in total DEGs(%)
100
80
60
40
20
0.0
186
193
5
453
461
16
Type I
Type II
Type III

Figure S2, related to Figure 3. Expression level of selected Interferon stimulated genes *in vivo* and *in vitro* mDCs.

(A) Gene expression intensity of indicated transcripts encoding selected RIG-I like receptors, antiviral effector genes and STAT transcripts in DC from ZIKV-infected individuals. Color coding reflects ratio of gene expression in ZIKV patients relative to controls.

(B) Heatmap reflecting the expression level of ISG differentially-expressed between *in vitro* infected DC and controls at indicated time points after infection. Corresponding data from *in vivo* DC from ZIKV patients are shown for comparison.

(C) Venn diagram showing overlaps between type I, type II and type III ISG that were differentially-expressed in *in vivo* infected mDCs relative to uninfected mDCs. Numbers in parentheses show the total number of ISGs from each class in current databases (Interferome v2.01).

(D) Waterfall plot representing the number of up-regulated and down-regulated type I, type II and type III ISG in *in vitro* infected mDCs relative to uninfected controls.

Figure S3

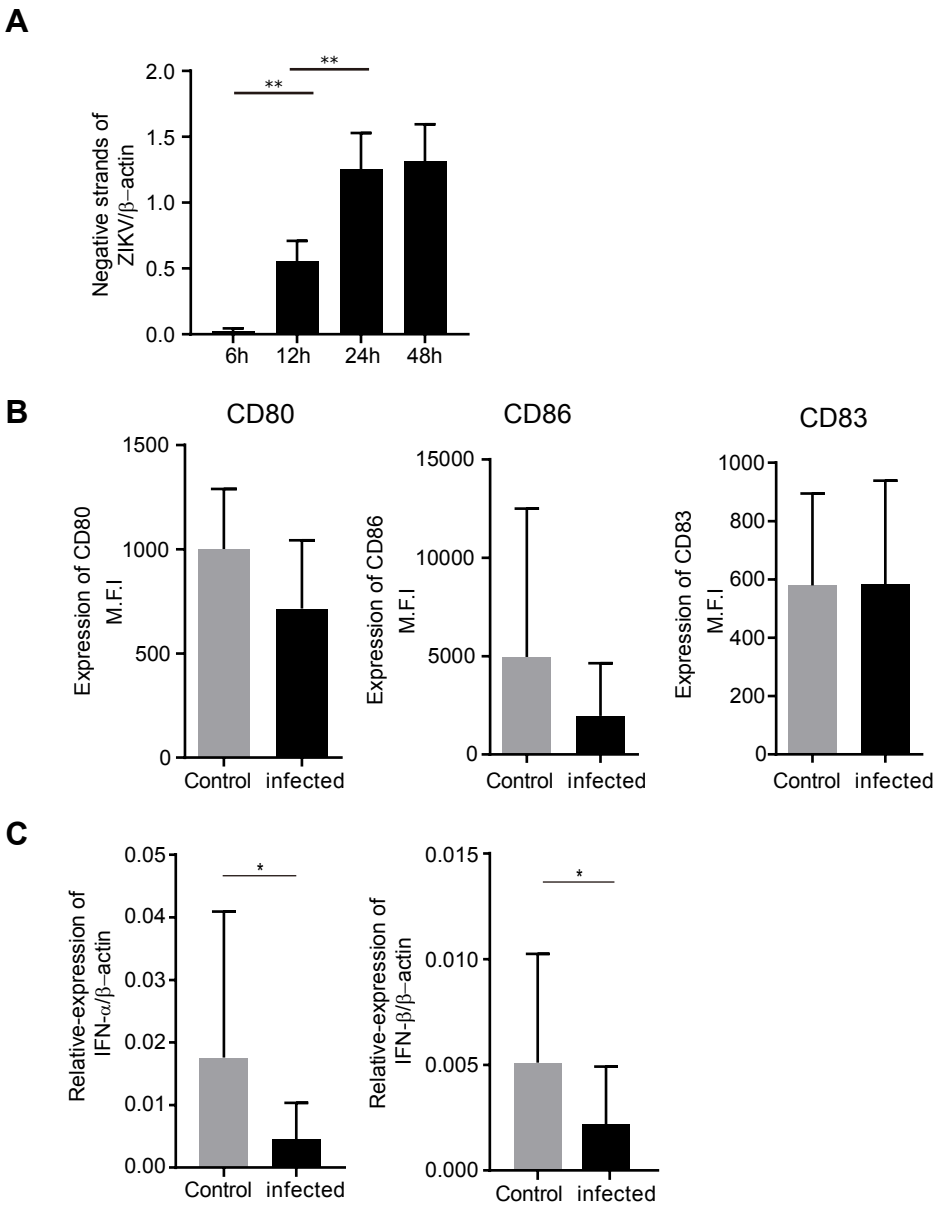
A
Negative strands of ZIKV/β−actin
2.0
1.5
1.0
0.5
0.0
**
**
6h
12h
24h
48h
B
CD80
CD86
CD83
Expression of CD80 M.F.I
Expression of CD86 M.F.I
Expression of CD83 M.F.I
1500
1000
500
0
15000
10000
5000
0
1000
800
600
400
200
0
Control
infected
C
Relative-expression of IFN-α/β−actin
Relative-expression of IFN-β/β−actin
0.05
0.04
0.03
0.02
0.01
0.00
0.015
0.010
0.005
0.000
*
*

Figure S3, related to Figure 4. Zika virus replication in *in vitro* infected monocyte–derived dendritic cells.

(A) Bar diagrams indicating the expression of negative-stranded ZIKV RNA in *in vitro* infected MDDCs at indicated timepoints after infection.

(B) Surface expression of indicated dendritic cell immune activation and maturation markers in ZIKV-infected MDDCs at 24h after infection.

(C) Relative expression of IFN-α and IFN-β transcripts from *in vitro* infected MDDCs samples measured by qPCR and normalized to beta-actin 24h after infection. Intra-individual differences were tested for statistical significance using Wilcoxon matched-pairs signed rank tests with post-hoc Dunn's test; * $p<0.05$; ** $p<0.01$.

Figure S4

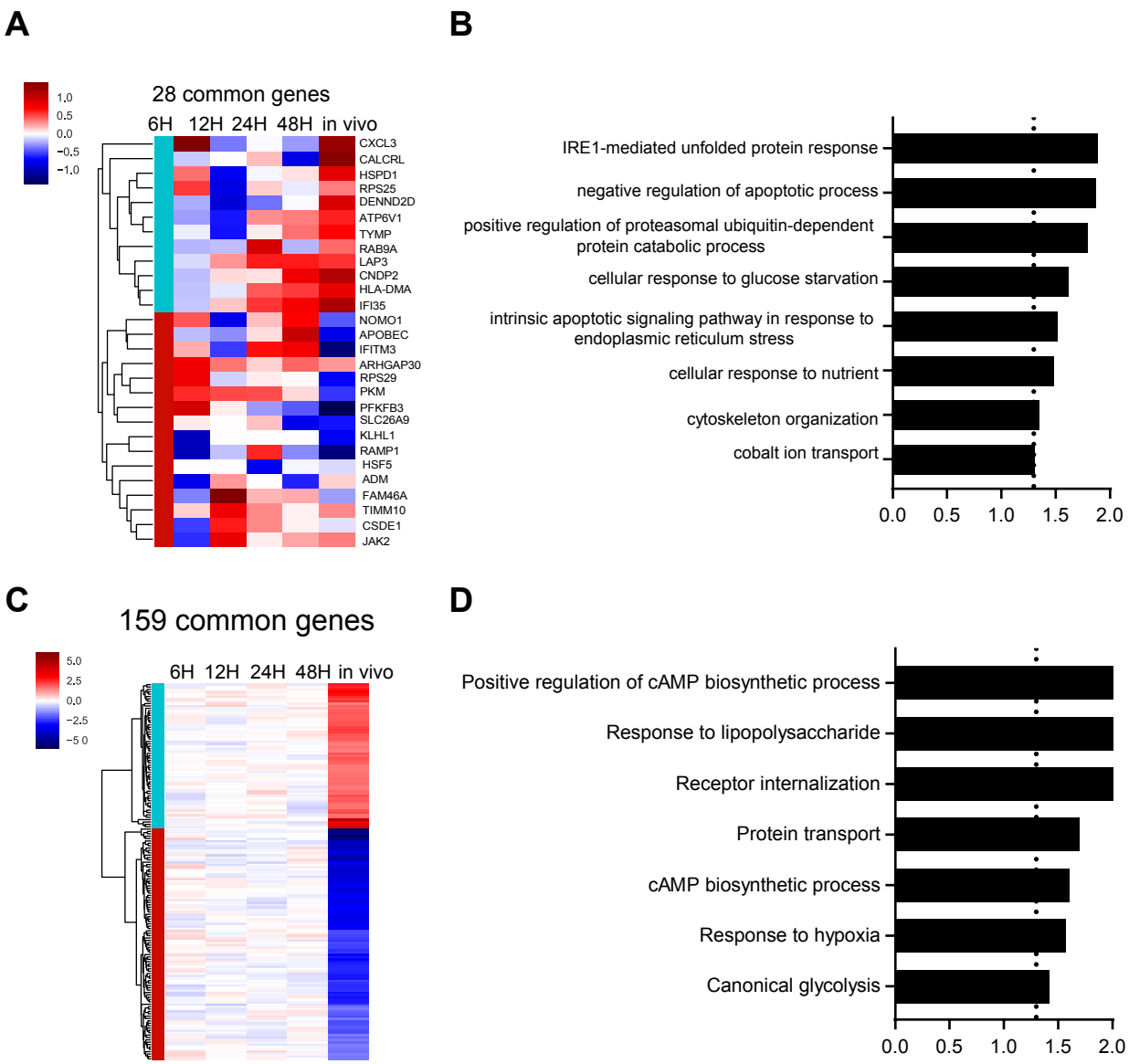
A
28 common genes
6H 12H 24H 48H in vivo
1.0
0.5
0.0
−0.5
−1.0
CXCL3
CALCRL
HSPD1
RPS25
DENND2D
ATP6V1
TYMP
RAB9A
LAP3
CNDP2
HLA-DMA
IFI35
NOMO1
APOBEC
IFITM3
ARHGAP30
RPS29
PKM
PFKFB3
SLC26A9
KLHL1
RAMP1
HSF5
ADM
FAM46A
TIMM10
CSDE1
JAK2
B
IRE1-mediated unfolded protein response
negative regulation of apoptotic process
positive regulation of proteasomal ubiquitin-dependent protein catabolic process
cellular response to glucose starvation
intrinsic apoptotic signaling pathway in response to endoplasmic reticulum stress
cellular response to nutrient
cytoskeleton organization
cobalt ion transport
0.0 0.5 1.0 1.5 2.0
C
159 common genes
6H 12H 24H 48H in vivo
5.0
2.5
0.0
−2.5
−5 0
D
Positive regulation of cAMP biosynthetic process
Response to lipopolysaccharide
Receptor internalization
Protein transport
cAMP biosynthetic process
Response to hypoxia
Canonical glycolysis
0.0 0.5 1.0 1.5 2.0

Figure S4, related to Figure 4. Analysis of overlaps between ZIKV dependency genes and DEGs from *in vitro* and *in vivo* infected DC.

(A) Heatmap representing the 28 transcripts shared between DEGs from *in vitro* infected DC and viral dependency genes defined by Savidis et al. Color coding reflects ratio of gene expression intensity *in vitro* infected samples and their respective controls; data from *in vivo* infected DC are shown for comparison.

(B) Functional annotations of 28 DEGs described in (A), as determined by DAVID v6.8.

(C) Heatmap representing 159 transcripts shared between DEGs from *in vivo* infected DC and the viral dependency genes described by Savidis et al. Color coding reflects ratio of gene expression intensity of *in vivo* infected samples and their respective controls; data from *in vitro* infected DC are shown for comparison.

(D) Functional annotations of transcripts described in (C), as determined using DAVID v6.8.

Figure S5

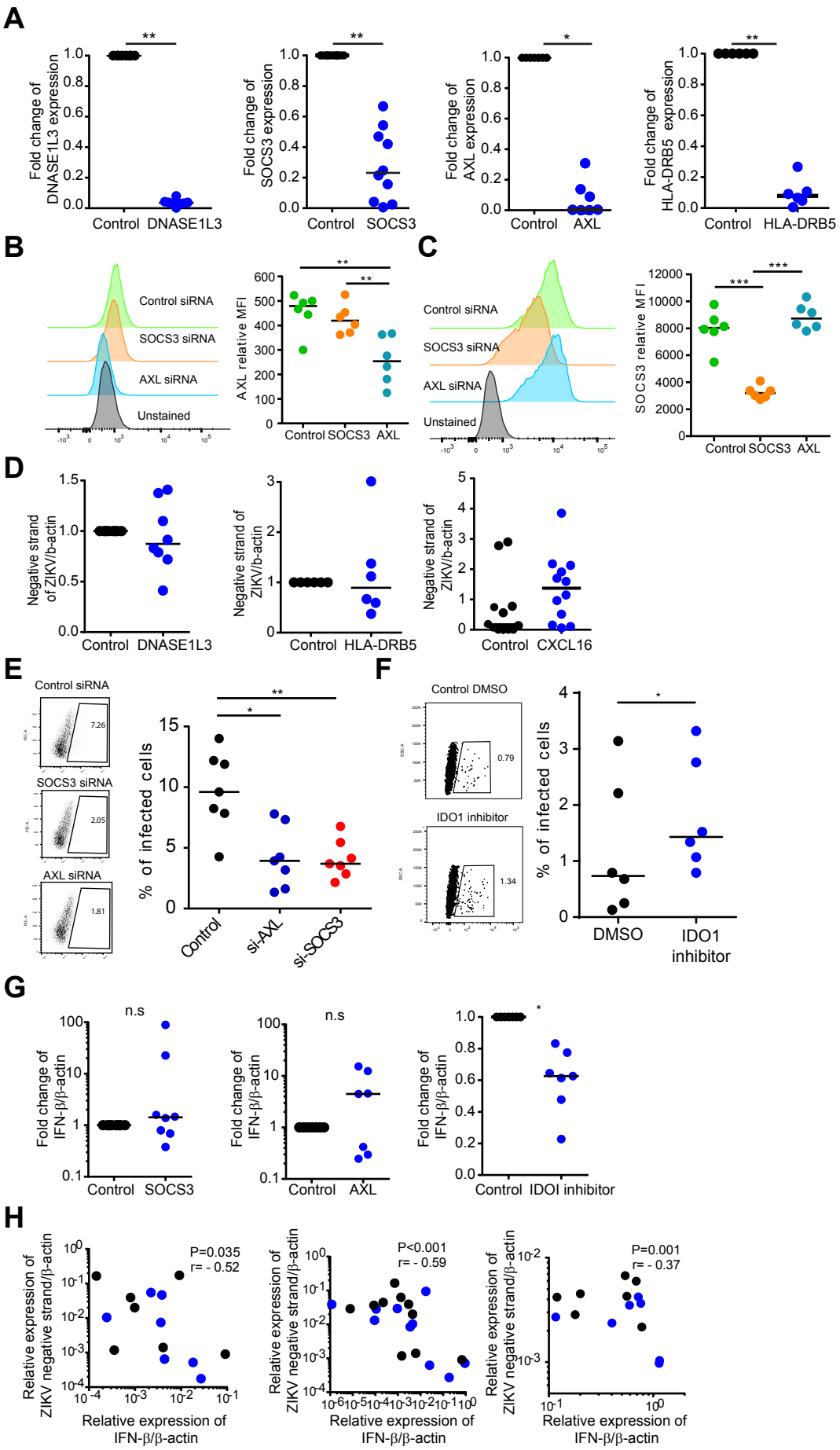
A
Fold change of DNASE1L3 expression
Control DNASE1L3
Fold change of SOCS3 expression
Control SOCS3
Fold change of AXL expression
Control AXL
Fold change of HLA-DRB5 expression
Control HLA-DRB5
B
Control siRNA
SOCS3 siRNA
AXL siRNA
Unstained
AXL relative MFI
Control SOCS3 AXL
C
Control siRNA
SOCS3 siRNA
AXL siRNA
Unstained
SOCS3 relative MFI
Control SOCS3 AXL
D
Negative strand of ZIKV/b-actin
Control DNASE1L3
Negative strand of ZIKV/b-actin
Control HLA-DRB5
Negative strand of ZIKV/b-actin
Control CXCL16
E
Control siRNA
SOCS3 siRNA
AXL siRNA
% of infected cells
Control
si-AXL
si-SOCS3
F
Control DMSO
IDO1 inhibitor
% of infected cells
DMSO
IDO1 inhibitor
G
Fold change of IFN-β/β-actin
n.s
Control SOCS3
Fold change of IFN-β/β-actin
n.s
Control AXL
Fold change of IFN-β/β-actin
Control IDOI inhibitor
H
Relative expression of ZIKV negative strand/β-actin
P=0.035
r= - 0.52
Relative expression of IFN-β/β-actin
Relative expression of ZIKV negative strand/β-actin
P<0.001
r= - 0.59
Relative expression of IFN-β/β-actin
Relative expression of ZIKV negative strand/β-actin
P=0.001
r= - 0.37
Relative expression of IFN-β/β-actin

Figure S5, related to Figure 4 and Figure 5. Effects of selected viral dependency genes on ZIKV replication and type I interferon secretion.

(A) Fold changes of DNASE1L3, HLA-DRB5 expression in MDDCs following siRNA-mediated gene silencing, relative to control samples.

(B) and **(C)** Efficiency of siRNA-mediated protein knock-down in MDDCs 48h after treatment with control (scramble) and AXL or SOCS3-specific siRNAs. Histogram shows a representative flow cytometry analysis of AXL (B) and SOCS3(C) expression on MDDCs and summary of the data was also shown (right panel).

(**D**) Fold changes of ZIKV negative-strand RNA after silencing of indicated gene transcripts in *in vitro* infected MDDCs. Data are normalized to control MDDCs.

(**E**) MDDCs were infected with ZIKV at MOI=1 after treatment with siRNA directed against AXL or SOCS3, or unspecific control siRNA. The supernatant was harvested 24h post-infection and co-cultured with the LLC-MK2 cell line. The proportion of infected MK2 cells was analyzed by flow cytometry using the 4G2 antibody after 72h of co-culture.

(**F**) MDDCs were infected with ZIKV at MOI=1 after treatment with 10nM of an IDO1 inhibitor (NLG-919) or control. The supernatant was harvested 24h post-infection and used to infect the LLC-MK2 cell line. The proportion of infected MK2 cells was analyzed by flow cytometry using the 4G2 antibody after 72h.

(G) Fold change of IFN-β after silencing/inhibiting indicated host transcripts in *in vitro* infected MDDCs. Data are normalized to control MDDCs.

(H) Correlations between the expression levels of IFN-β and the corresponding levels of ZIKV negative strand RNA levels after silencing SOCS3 (left), silencing AXL (middle) or addition of 100mM of the IDO1 inhibitor NLG99 (right). Cumulative data were analyzed using generalized estimated equations adjusted for repeated measures.

Table S1, related to Figure1 and Figure 4-5. Primer sequences in this study

Number	Name	Sequence
1	ZK1086-F	CCGCTGCCCAACACAAG
2	ZK1162-R	CCACTAACGTTCTTTTGCAGACAT
3	ZK1107-FAM	/56-FAM/AGCCTACCT/ZEN/TGACAAGCAGTCAGACACTCAA/31ABkFQ/
4	HLADRB5-F	GCAGCAGGATAAGTATGAGTGT
5	HLADRB5-R	GCAAGTCCTCCTCTTGGTTATAG
6	DNASE1L3-F	AGCCCTTTGTGGTCTGGTTC
7	DNASE1L3-R	CGTCCGTGTAGACCTCAACC
8	SOCS3-F	GGAGACTTCGATTCGGGACC
9	SOCS3-R	GGTACTCGCTCTTGGAGCTG
10	AXL-F	AACCTTCAACTCCTGCCTTCTCG
11	AXL-R	CAGCTTCTCCTTCAGCTCTTCAC
12	Tryosine-F	GCAAGCCTTTGACAGTGTCATGG
13	Tryosine-R	GTTCATCGCTGATGCCCAAGCT
14	Mer-F	CAGGAAGATGGGACCTCTCTGA
15	Mer-R	GGCTGAAGTCTTTCATGCACGC
16	TIM-1-F	GCTTTGCAAAATGCAGTTGA
17	TIM-1-R	TGTTGGAATGCCAGATGAAA
18	TIM-3-F	GACTTCACTGCAGCCTTTCC
19	TIM-3-R	GATCCCTGCTCCGATGTAGA
20	TIM-4-F	GGATTTGTGCTCTTCGCATT
21	TIM-4-R	CCCCCATCCTCAATCTAACA
22	IFN-alpha-F	GCTTTACTGATGGTCCTGGTGGTG
23	IFN-alpha-R	GAGATTCTGCTCATTTGTGCCAG
24	IFN-beta-F	GAATGGGAGGCTTGAATACTGCCT
25	IFN-beta-R	TAGCAAAGATGTTCTGGAGCATCTC
26	Env-standard curve-F	TAATACGACTCACTATAGGGGCTCAACGAGCCAAAAAGTC
27	Env-standard curve-R	GTCGTGGAACCACTCCTTGT

Table S2, related to Figure 2. Ingenuity Pathways Analysis of DEGs from *in vivo* infected DC.

Normalized data for DEGs and ISGs identified in *in vivo* infected DC, as determined by Ingenuity Pathways Analysis of canonical pathways and disease & functions. Relevant pathways and disease functions for mDCs are highlighted in light green.

Table S3, related to Figure 2. Ingenuity Pathways Analysis of DEGs from *in vitro* infected DC.

Normalized data for DEGs from *in vitro* infected DC, as determined by Ingenuity Pathways Analysis of canonical pathways for each indicated time point after infection.

Table S4, related to Figure 2. Analysis of DEGs overlapping between *in vivo* and *in vitro* infected DC.

Ingenuity Pathways Analysis of canonical pathways of the 199 genes shared between DEGs from *in vitro* and *in vivo* infected DC. Relevant pathways for mDCs are highlighted in light green

Table S5, related to Figure 3. Functional categories of the 69 pre-defined antiviral ISGs that were differentially expressed in *in vivo* infected mDCs.

Table S6, related to Figure 4. Viral dependency genes.

List of the DENV or ZIKV viral dependency genes overlapping with DEGs detected in *in vitro* and *in vivo* infected DC.

Supplemental Experimental procedures

Flow cytometry and cell sorting

PBMCs or CBMCs were stained with antibodies against CD3 (clone OKT3), CD4 (clone OKT4), CD8 (clone SK1), CD19 (clone HIB19), CD56 (clone HCD56), CD16 (clone B73.1), CD14 (clone HCD14), HLA-DR (clone L243), CD11c (clone 3.9), CD123 (clone 6H6) and Blue viability dye (BVD), washed with PBS, and subjected to flow cytometry using a FACS LSR Fortessa (BD Biosciences) or live cell sorting of CD4 T cells ($CD3^+$ $CD4^+$), CD8 T cells ($CD3^+$ $CD8^+$), monocytes ($CD3^-$ $CD19^-$ $CD14^+$), NK cells ($CD3^-$ $CD19^-$ $CD14^-$ $CD56^+$), B cells ($CD3^-$ $CD14^-$ $CD19^+$), plasmacytoid dendritic cells ($CD3^-$ $CD14^-$ $CD19^-$ $CD56^-$ $HLADR^+$ $CD11c^-$ $CD123^+$) and mDCs ($CD3^-$ $CD14^-$ $CD19^-$ $CD56^-$ $HLADR^+$ $CD11c^+$ $CD123^-$) using a FACS Aria cell sorter (BD Biosciences) at 70 pounds per square inch. Cell sorting was performed by the Ragon Institute Imaging Core Facility and resulted in the isolation of these 7 subsets with the defined phenotypic characteristics of >95% purity. PBMCs and monocyte-derived dendritic cells (MDDCs) were stained with antibodies against Lineage (clones UCHT1, HCD14, 3G8, HIB19, 2H7, HCD56), CD14 (clone HCD14), CD80 (clone L307.4), CD83 (clone HB15e), CD86 (clone IT2.2), washed with PBS, and subjected to flow cytometry using a FACS LSR Fortessa (BD Biosciences). Total ROS production was measured using 1μM of the CM-H2DCFDA probe (Thermo Fisher Scientific) according to the product manual. Phorbol 12-myristate 13-acetate (PMA) was served as positive control and DMSO only as negative control.

Generation of Monocyte-derived dendritic cells

Approximately 2×10^8 PBMCs were plated in fresh RPMI1604 medium plus 10% FBS (R10) and incubated 2 hours at 37°C to adhere monocytes. After discarding non-adherent cells, cells were washed two times with pre-warmed PBS. Monocytes were differentiated into MDDCs using fresh R10 complete medium supplemented with 100 ng/ml of GM-CSF (PeproTech) and 50 ng/ml IL-4 (PeproTech). Fresh culture medium was added at day 3 and MDDCs were harvested at day 5 (Nair et al., 2012).

Transcriptional profiling of primary mDCs

Total RNA was extracted from sorted cell populations using a commercial PicoPure RNA Isolation Kit **(**Thermo Fisher Scientific). RNA-Seq libraries from isolated dendritic cells from each group were generated as previously described (Trombetta et al., 2014). Briefly, whole transcriptome

amplification (WTA) and tagmentation-based library preparation was performed using SMART-seq2, followed by sequencing on a NextSeq 500 Instrument (Illumina). The quantification of transcript abundance was conducted using RSEM software (v1.2.22) supported by STAR aligner software (STAR_2.4.2a). The raw reads were aligned to Hg38 human genome database. To detect differentially expressed genes (DEGs); the Bioconductor/R-project package with DESeq2 was used to calculate FDR-adjusted p-values. Ingenuity Pathway Analysis (IPA) was used to functionally categorize differentially expressed genes.

Cells

LLC-MK2 and C6/36 cells were obtained from ATCC and maintained in complete DMEM medium (Sigma) supplemented with 10% fetal bovine serum, 2mM L-Glutamine (Corning), 1mM HEPES (Corning), and 1x Penicillin-Streptomycin Solution (Corning). MDDCs, PBMCs, and CBMCs were maintained in a complete R10 medium including RPMI 1640 medium (Sigma) supplemented with 10% fetal bovine serum, 2mM L-Glutamine (Corning), and 1x Penicillin-Streptomycin Solution (Corning).

Zika virus production and titration

ZIKV Strain PRVABC59 was isolated from a patient who travelled to Puerto Rico in 2015 (Lanciotti et al., 2016). The virus was produced using the Vero cell line and was kindly provided by the US Centers for Disease Control (CDC) in February 2016. The virus was propagated only once in our lab using the C6/36 cell line. Viral stocks were titrated by flow cytometry on LLC-MK2 cells using 4G2 antibody (Novus Biologicals) which recognize a conserved epitope on the E protein of the Flaviviruses family and stored at -80°C in DMEM with 10% FBS.

ZIKV infection of cells

For *in vitro* infection, PBMCs and CBMCs cells were infected with ZIKV at a multiplicity of infection (MOI) of 1. The cells were incubated for 2 h at 37°C. Next, the inoculum was removed and the cells were washed four times with PBS. Culture medium was added to each well, and the cells were incubated at 37°C and 5% CO_2 for the duration of the experiment. Subsets of cells, including CD4 T cells, CD8 T cells, monocytes, NK cells, pDCs, B cells, and mDCs were then sorted by FACS as described above. For MDDCs infection, cell numbers were counted and infected by the same procedure as described for PBMCs and CBMCs. To confirm the permissiveness to ZIKV of each subset, we sorted T cells, monocytes, NK, B cells and mDCs and

infected cells as described above. The proportion of infected cells was accessed by flow cytometry using an antibody recognizing the ZIKV E protein (clone 4G2).

ZIKV qRT-PCR and qPCR

Total RNA was extracted from indicated cell populations by PicoPure RNA Isolation Kits according to the manufacturer's protocol. cDNA was generated with random primers according to standard procedures using Superscript III kit. qRT-PCR was performed using QuantiTect Probe RT-PCR kit (Qiagen) according to the manufacturer's instructions. ZIKV primers are listed in supplemental Table S1 and beta-actin primers (Hs0160665_g1) served as controls. qPCR for detection of AXL, SOCS3, HLA-DRB5, DNASE1L3, IFN-α, IFN-β, TIM and TAM receptors (see primer sequence in Table S1) was performed using the QuantiTect SYBR Green PCR Kit (Qiagen). In addition, the expression of genes involved in flavivirus replication was assessed using the Flaviviridae Infections R384 plate (Bio-Rad) and the data were visualized by PrimePCR™ Analysis Software. All qRT-PCR and the qPCR reaction were run by an Applied Biosystems Vii7 real-time PCR system (Applied Biosystems).

Analysis of negative-stranded ZIKV mRNA

Total viral RNA from ZIKV-infected C6/36 cells was purified using a PicoPure RNA Isolation kit following the manufacturer's protocol. A standard RT-PCR was then carried out by using primers containing the T7 promoter sequence as listed in Table S1. The PCR product was used to generate ZIKV RNA fragments by *in vitro* transcription using a MAXIscript kit (Ambion, Austin, TX). Negative strand viral cDNA was generated with forward primers as listed in Table S1, using the superscript III kit (Invitrogen, USA). Copies of viral RNA were quantified by normalizing each sample's threshold cycle (*CT*) value to a ZIKV RNA standard curve obtained as described before (Hamel et al., 2015).

siRNA-mediated gene knockdown

Silencing of AXL, SOCS3, HLA-DRB5, DNASE1L3 or scramble control using siRNA pools (purchased from On-TARGET plus SMARTpool, Dharmacon) were performed by nucleofection of MDDCs (program CM120, Amaxa 4D-Nucleofector, Lonza) with P3 Primary Cell 4D-Nucleofector® X Kit according to the manufacturer's instructions. Nucleofected MDDCs were infected with ZIKV after 48 hours, type I IFN responses and negative-stranded ZIKV RNA were subsequently analyzed at 24-hour post-infection by qPCR. The efficiency of siRNA-mediated gene

knockdown was determined at the mRNA level by qPCR and at the protein level by flow cytometry using antibodies against AXL (APC conjugated, R&D Systems, USA) and SOCS3 (Abcam, USA). To assess intracellular SOCS3 protein expression, cells were fixed, permeabilized and stained with a primary rabbit anti-human SOCS3 (Abcam, USA), followed by labeling with a secondary anti-rabbit FITC antibody (Biolegend, USA).